J. Am. Soc. Mass Spectrom. (2011) 22:1941–1952
DOI: 10.1007/s13361-011-0228-3

RESEARCH ARTICLE

Characterizing the Intramolecular H-bond and Secondary Structure in Methylated GlyGlyH$^+$ with H_2 Predissociation Spectroscopy

Christopher M. Leavitt,[1] Arron B. Wolk,[1] Michael Z. Kamrath,[1] Etienne Garand,[1] Michael J. Van Stipdonk,[2] Mark A. Johnson[1]

[1]Sterling Chemistry Laboratory, Yale University, P.O. Box 208107, New Haven, CT 06520, USA
[2]Department of Chemistry, Wichita State University, 1845 Fairmount Ave., Wichita, KS 67208, USA

Abstract

We report vibrational predissociation spectra of the four protonated dipeptides derived from glycine and sarcosine, GlyGlyH$^+$•$(H_2)_{1,2}$, GlySarH$^+$•$(D_2)_2$, SarGlyH$^+$•$(H_2)_2$, and SarSarH$^+$•$(D_2)_2$, generated in a cryogenic ion trap. Sharp bands were recovered by monitoring photoevaporation of the weakly bound H_2 (D_2) molecules in a linear action regime throughout the 700–4200 cm^{-1} range using a table-top laser system. The spectral patterns were analyzed in the context of the low energy structures obtained from electronic structure calculations. These results indicate that all four species are protonated on the N-terminus, and feature an intramolecular H-bond involving the amino group. The large blue-shift in the H-bonded N–H fundamental upon incorporation of a methyl group at the N-terminus indicates that this modification significantly lowers the strength of the intramolecular H-bond. Methylation at the amide nitrogen, on the other hand, induces a significant rotation (~110°) about the peptide backbone.

Key words: Vibrational spectroscopy, Cryogenic ions, Peptides, Electrospray ionization, Intramolecular hydrogen bond, Secondary structure

Introduction

Understanding the structures, energetics, and decomposition pathways of the gas phase ions derived from peptides and proteins is central to the widely used "bottom-up" approach for proteome sequencing [1, 2]. An important overall goal of such studies is to expand the sequence coverage available in proteomic analyses by rationalizing the fragmentation pathways [e.g., observed in collision-induced dissociation (CID)] in a structural context [3–7]. Vibrational spectroscopy is emerging as a powerful means with which to elucidate such structures by revealing peptide conformations and protonation sites through theoretical analysis of the observed band patterns [8–27]. This spectroscopic data is most often available through the integration of tunable infrared laser photodissociation with mass spectrometry and, in most cases, spectra of the mass-selected ions are obtained under ambient temperature conditions using infrared multiple photon dissociation (IRMPD) [28–33]. A recent variation on this scheme [34], yielding a resolution enhancement of 5 to 10 times that which is typically reported, involves cooling the ions close to 10 K [35–37] and "tagging" them with a weakly bound mass "messenger" using cryogenic ion trapping techniques [38–40]. The resulting spectra are obtained in a linear regime that is readily compared with calculated band patterns for ions frozen into their zero-point energy levels. Here we study the

Electronic supplementary material The online version of this article (doi:10.1007/s13361-011-0228-3) contains supplementary material, which is available to authorized users.

Correspondence to: Michael J. Van Stipdonk; *e-mail:* mike.vanstipdonk@wichita.edu, Mark A. Johnson; *e-mail:* mark.johnson@yale.edu

Received: 31 May 2011
Revised: 3 August 2011
Accepted: 3 August 2011
Published online: 27 August 2011

family of protonated dipeptides indicated in Figure 1 using the H_2 tagging approach [41, 42]. We choose this series of ions because it allows us to determine the changes that occur when the N–H motif is changed to N-CH_3 at both the N-terminus and amide positions.

The protonated diglycine ion has been investigated previously using FTMS [43–45], IRMPD [18], and H_2 tagging approaches [34], and there is a consensus that the protonation site is located at the N-terminus. Although several isomers were invoked to explain the room temperature IRMPD spectrum, the sharper bands recovered in the 10 K H_2 tagged spectrum could be assigned in the context of a dominant, fully extended "all trans" conformer, which was identified as the lowest energy isomer by Wu et al. [18]. Starting with this well-defined $GlyGlyH^+$ structure, the present paper explores the structural changes induced by methyl substitution at the amide group ($GlySarH^+$), at the N-terminus ($SarGlyH^+$), and at both positions ($SarSarH^+$). Sharp bands, ranging from 7 to 30 cm^{-1} FWHM, were recovered in all cases, and the resulting patterns were analyzed in the context of minimum energy structures and their predicted harmonic spectra. The qualitative character of the strongly anharmonic motions associated with the intramolecular H-bonds was also addressed by calculating the shapes of the potential surfaces describing the large amplitude displacements of the shared protons between donor (N) and acceptor (O) atoms.

Experimental

Cryogenic ion Photofragmentation Instrumentation

Infrared spectra were recorded on the Yale tandem time-of-flight photofragmentation mass spectrometer, which has recently been fitted with an electrospray ionization (ESI) source coupled to a cryogenic, quadrupole ion trap designed closely after that of Wang et al. [46] and described in detail previously [47]. Millimolar solutions of GlyGly and its methylated derivatives were prepared by dissolving the solids in a mixture of methanol, water, and 0.1% formic acid in a volume ratio of 49.5:49.5:1. The solutions were electrosprayed from a ground silica capillary with a 15 μm tip (New Objective, Woburn, MA, USA) held at +2000 V, and the ions were injected into the apparatus through a heated stainless steel capillary (~80 °C). The desolvated ions were then transferred through four differentially pumped stages (1, 0.2, 10^{-4}, 10^{-7} mbar) in RF-only ion guides. After 90° deflection by a static turning quadrupole, the ions were focused and collected in a 3D quadrupole ion trap (Jordan, Grass Valley, CA, USA).

The ion trap was cooled with a closed-cycle helium cryostat (Janis Research, Wilmington, MA, USA) and held at ~10 K with a thermostat-controlled 100 W heater. The ions accumulate in the trap with the aid of a pulsed collision gas mixture composed of 20% H_2 (or D_2) in a balance of He. The gas was introduced through a pulsed valve (Parker Hannifin, Cleveland, OH, USA Series 99) with a backing pressure of 1 bar and a pulse length of 1 ms. Introduction of a delay before ion extraction, ranging from 30 to 90 ms, was found to be crucial in the tagging process. During operation the pressure of the main vacuum envelope increased from $\sim 3\times10^{-7}$ to $\sim 1\times10^{-6}$ mbar, and was empirically optimized for production of H_2 adducts.

After formation of the molecular adducts, ions were ejected from the trap using a push/pull voltage pulse (+90 V/–90 V) and directed into the extraction region of a Wiley-McLaren TOF mass spectrometer. At the first temporal focus, the mass-selected ions were intersected with the output from an OPO/OPA IR laser (LaserVision, Bellevue, WA, USA) pumped by a Nd:YAG laser (7 ns, 10 Hz). Spectra were collected over the

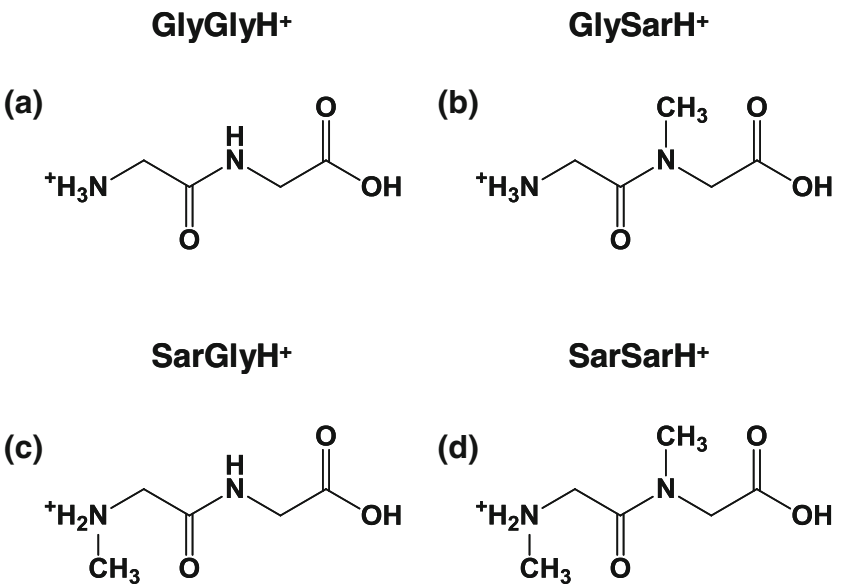

Figure 1. Schematic structures of the four dipeptides characterized in this study: **(a)** $GlyGlyH^+$, **(b)** $GlySarH^+$, **(c)** $SarGlyH^+$, and **(d)** $SarSarH^+$

range 700 to 4200 cm^{-1}. The lower frequency coverage (700–2500 cm^{-1}) was obtained using an additional mixing stage in which the 3 μm and 1.5 μm beams from the output of the OPO/OPA system were combined in an external $AgGaSe_2$ crystal. As a result of this extra nonlinear process, the bandwidth increases from approximately 3 cm^{-1} in the high energy range to 6 cm^{-1} in the lower energy range.

The ionic photofragment intensity corresponding to loss of one or two hydrogen molecules (as indicated in figure captions) was monitored versus photon energy to generate the action spectra. The fragment intensity was also normalized to the laser pulse energy to account for power fluctuations over the large photon energy range of the scan. Pulse energies were kept below 5 mJ to prevent saturation effects. To ensure that the spectra correspond to the single-photon action regime, the laser pulse energies were adjusted so as to achieve a linear photofragmentation yield for excitation at the resonances with the highest photofragment intensities. In the $GlySarH^+$ and $SarSarH^+$ cases (displayed in Figure 2b and d, respectively), molecular deuterium was used as a tag because the heavier D_2 affords greater separation between parent and daughter ions in the secondary stage of mass selection. This increased separation minimizes the overlap between the two ion packets and

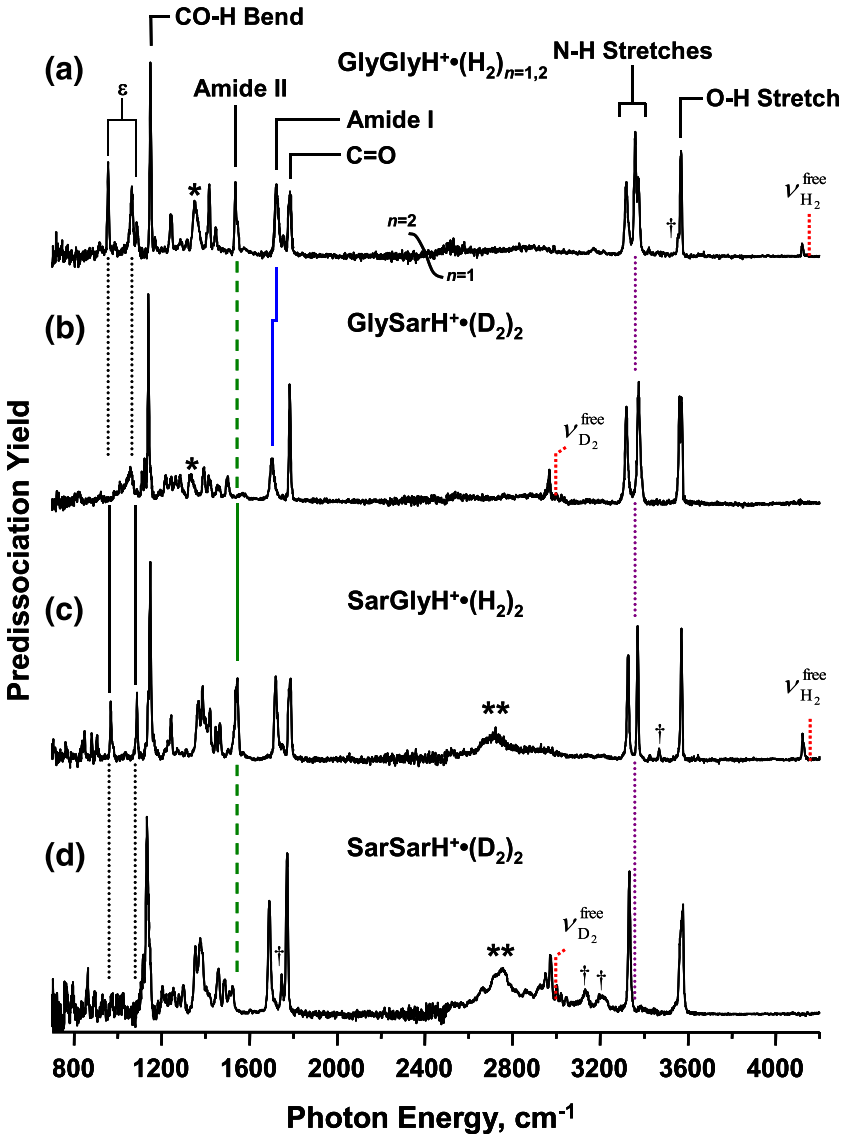

Figure 2. Vibrational predissociation spectra of **(a)** $GlyGlyH^+•(H_2)_2$ for photon energies below 2450 cm^{-1}, and $GlyGlyH^+•H_2$ above 2450 cm^{-1}; **(b)** $GlySarH^+•(D_2)_2$; **(c)** $SarGlyH^+•(H_2)_2$, and **(d)** $SarSarH^+•(D_2)_2$, in all cases collected by monitoring the photoproduction of the bare protonated dipeptides. The singly tagged adduct in **(a)** was selected in the high energy range to reveal all three N–H stretches, two of which are accidentally overlapped in the $GlyGlyH^+•(H_2)_2$ complex (see Figure S1). Bands associated with the intramolecular H-bond in the major isomer are indicated by (*) and (**) for the peptides containing primary and secondary protonated amines, respectively. Minor transitions that are tentatively assigned to contributions from additional isomers are indicated by (†)

brings the experiment closer to a "zero background" situation. No appreciable changes in the spectra were observed when H_2 was replaced by D_2 in the adducts, as evidenced by the comparison between the $GlyGlyH^+•(D_2)_2$ and $GlyGlyH^+•(H_2)_2$ spectra presented in Figure S2.

Synthetic Details

The dipeptides were prepared using standard solid-phase peptide synthetic techniques, using FMOC-protected amino acids and FMOC-glycine or FMOC-sarcosine loaded Wang resin. Finished dipeptides were cleaved from resin using trifluoroacetic acid, separated from resin by vacuum filtration and used without further purification.

Computational Details

The Biological and Organic Simulation System (BOSS) was used to survey the conformational space of the protonated peptides [48]. A Monte Carlo searching algorithm was utilized in a modified script provided with the software suite. Using 30,000 steps and an r_{rms} tolerance of 0.3 Å, between 60 and 600 distinct conformers were obtained for each starting structure. Both the N-terminus and amide carbonyl oxygen were protonated in preliminary structures. All conformers within 12 kJ/mol of the global minimum were then optimized using the Gaussian 09 software package [49]. The protocol for this involved initial optimizations using the B3LYP/6-31G* method. Then, starting with these refined structures, optimizations and harmonic frequency calculations were independently carried out using both the MP2/6-311+G(d,p) and B3LYP/6-311+G(d,p) methods and basis. For simplicity we report the zero-point corrected relative energies calculated at the MP2 level (Table 1) with the B3LYP energies tabulated in supplemental information (Table S1). These two methods returned the same five lowest energy conformers with only one exception (the fifth lowest energy conformer of $SarSarH^+$), but the relative energies of the conformers were method-dependent. To facilitate discussion involving alternative isomers for the various species, we adopt the naming scheme $[Peptide]H^+(X)$, with X indicating the energy ranking of the given peptide recovered using the MP2 method. For the MP2/6-311+G(d,p) calculated (harmonic) spectra, the low energy range (700–2450 cm^{-1}) was scaled by 0.977, the upper tolerance of the scaling factor for that method and basis listed in the NIST Webbook [50]. For the high energy range (2450–3800 cm^{-1}), the frequencies were scaled by the factor that brought the free OH band of the lowest energy isomer into agreement with experiment (0.943 for $GlyGlyH^+$, 0.944 for $GlySarH^+$, 0.943 for $SarGlyH^+$, and 0.945 for $SarSarH^+$).

Results and Discussion

Survey of the Photodissociation Spectra

Figure 2 presents a survey of the vibrational predissociation spectra obtained for the four peptides central to this study. The IRMPD and H_2-tagged spectra of $GlyGlyH^+$ have been reported earlier, [18, 34] and the H_2-tagged spectrum reveals many relatively sharp (~10 cm^{-1} FWHM) vibrational band origins underlying the more diffuse IRMPD envelopes. The linewidths of the H_2-tagged spectra vary from 7 to 30 cm^{-1} over the scans, with the narrowest lines scattered throughout and occurring with values on the same order as the laser bandwidth (~6 cm^{-1} below 2400 cm^{-1}).

All four dipeptides display a weak band derived from the molecular tag (H_2 or D_2), which falls just slightly below the nominally forbidden transition of the isolated diatomic molecules (red dotted lines in Figure 2), consistent with their roles as minimally invasive mass "messengers." Our previous report [34] established that the binding energy for attachment of molecular hydrogen to $GlyGlyH^+$ is about 500 cm^{-1}, and that the binding occurs preferentially to the N–H groups on the N-terminus in a T-shaped arrangement. Specifically, calculations indicate that the N–H bond lies perpendicular to the H_2 intramolecular axis, with the donor hydrogen atom pointing toward the midpoint of the H_2 bond.

The O–H stretches associated with the free acid functionality of the peptides occur in an isolated region near 3600 cm^{-1}, while the multiplet due to the N–H stretches appears just below it around 3400 cm^{-1}. The next sharp bands with appreciable intensity in all systems occur much lower in energy, with the acid C=O stretch at ~1800 cm^{-1} and the amide I band near 1700 cm^{-1}. The lowest energy feature common to all species is the CO–H bend due to the carboxylic acid group near 1150 cm^{-1}. These signature features, as well as a few lower energy transition energies, are collected in Table 2 for the four ions.

Table 1. The Zero-Point Corrected Energies (MP2/6-311+G(d,p)) of the Five Lowest Energy Conformers for the Dipeptides Characterized in this Study. All Values are Reported Relative to the Lowest Energy Conformation. Corresponding Structures can be Found in Supplemental Figures S2, S4, S6, and S8

	ΔE (kJ/mol)			
	Species			
Conformer	$GlyGlyH^+•(H_2)_{1,2}$	$GlySarH^+•(D_2)_2$	$SarGlyH^+•(H_2)_2$	$SarSarH^+•(D_2)_2$
1	0	0	0	0
2	0.3	0.6	4.6	1.4
3	3.3	0.9	4.7	2.8
4	5.3	3.4	6.0	3.2
5	5.8	3.5	9.5	17.6

Table 2. Vibrational Band Positions (±5 cm^{-1}) Recovered for the Four Peptides Characterized in this Work Over the 700–4200 cm^{-1} Range

Species	Frequencies, cm^{-1}									
	Extended Breathing Modes		CO-H bend	Amide II	Amide I	C=O	Sym. NH_2	Amide NH	Asym. NH_2	O-H stretch
	ε^a	ε^b								
$GlyGlyH^+\cdot(H_2)_{1,2}$	954	1065	1148	1536	1722	1786	3319	3360	3373	3569
$GlySarH^+\cdot(D_2)_2$	-	-	1139	-	1700	1783	3319	-	3375	3561, 3569
$SarGlyH^+\cdot(H_2)_2$	967	1087	1147	1545	1721	1788	3328*	3370	-	3570
$SarSarH^+\cdot(D_2)_2$	-	-	1139	-	1697	1754, 1778	3333*	-	-	3563, 3574

*Methylation on the amino terminus in $SarGlyH^+$ and $SarSarH^+$ results in a largely decoupled motion of a single NH group

Several qualitative aspects of the spectral evolution displayed in Figure 2 are evident by inspection. For example, because the amide II band near 1535 cm^{-1} is mostly derived from the embedded N–H wag, replacement of this hydrogen atom by CH_3 should remove this band from the spectrum. Note that $GlySarH^+$ and $SarSarH^+$ ions feature methyl substitution at the amide-N position, and indeed both of their spectra (Figure 2b and d, respectively) display a dramatic reduction of intensity in the amide II signature region. The free N–H stretches are also informative in that the intermediate transition near 3360 cm^{-1} disappears in the $SarSarH^+$ spectrum (the purple dotted line in Figure 2d). This behavior suggests that only one of its two hydrogen atoms on the amino group is non-bonded, which in turn indicates the formation of an intramolecular H-bond. We note that two sharp bands located just below the C–OH bend transition near 1150 cm^{-1} only appear when a hydrogen atom resides on the amide N–H location (ε in traces 2a and 2c), suggesting that differing skeletal motifs may be in play whether or not a methyl group resides at this site. Finally, peptides with a sarcosine residue present at the N-terminus exhibit a new diffuse feature centered at 2700 cm^{-1} (Figure 2c and d), with weaker structure tailing toward the high energy side of the main peak.

To extract more quantitative structural details, we next consider the spectra in the context of the harmonic vibrational

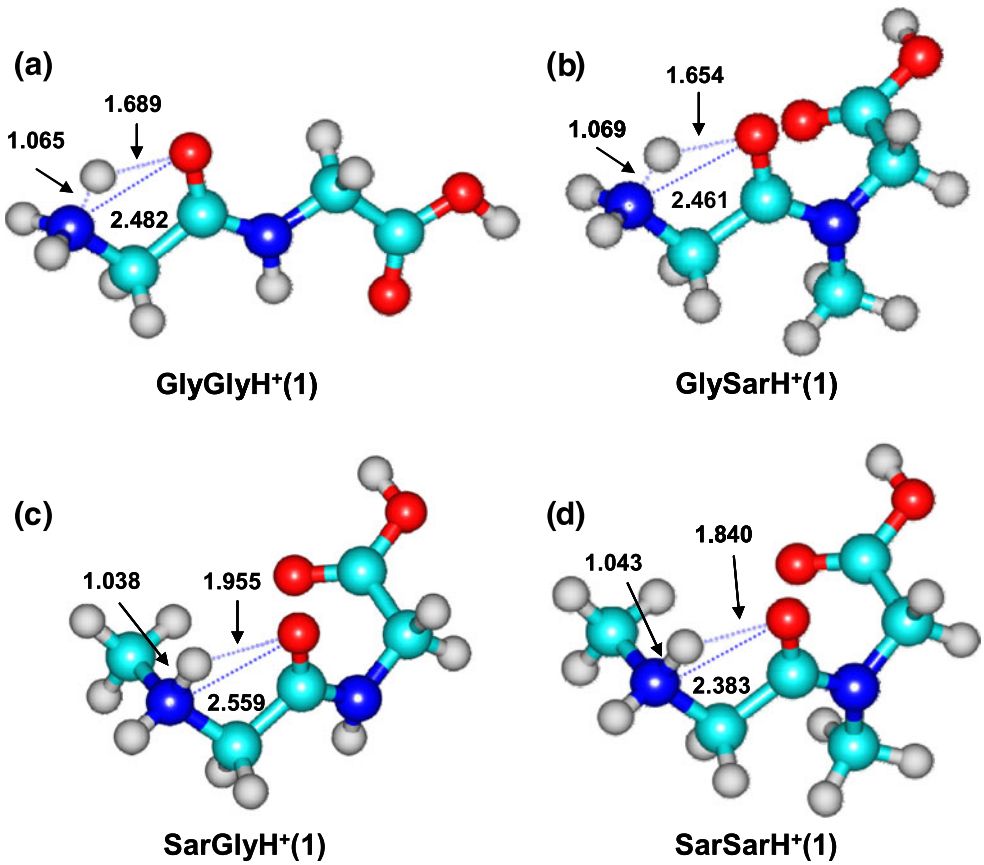

Figure 3. The MP2/6-311+G(d,p) optimized geometries of the lowest energy conformers of **(a)** $GlyGlyH^+$, **(b)** $GlySarH^+$, **(c)** $SarGlyH^+$, and **(d)** $SarSarH^+$. The peptides are labeled using the scheme $[Peptide]H^+(X)$, where X indicates the energy rank of the isomers. Since these are all lowest energy minima, X=1 for all four structures

patterns expected for various calculated isomers. Figure 3 presents the lowest energy MP2 structures for all four dipeptides, with the $GlyGlyH^+(1)$ conformer identical to that reported earlier by McMahon and Wu [18]. Note that all lowest energy forms accommodate the extra proton on the N-terminus, and one of the amine hydrogen atoms is H-bonded to the amide carbonyl group with distances between the shared proton and acceptor atom (H and O, respectively) lying in the 1.6–2.0 Å range. We expect that this H-bonded N–H stretch will be significantly red-shifted owing to substantial anharmonicity in the potential surface describing translocation of the proton between N and O sites, both of which support local minima as described in detail below.

$GlyGlyH^+$ and $GlySarH^+$

Figure 4 compares the experimental photodissociation spectrum of $GlyGlyH^+\bullet(H_2)_{1,2}$ with the calculated (MP2/6-311+G(d,p)) harmonic spectrum corresponding to the $GlyGlyH^+(1)$ structure shown in Figure 3a. This system has already been discussed at length in an earlier publication, [34] and its bands have been analyzed in the context of the fully extended $GlyGlyH^+(1)$ structure. Just below 3400 cm^{-1}, the three N–H stretches lie close together with the symmetric and asymmetric NH_2 modes of the amine bracketing the amide N–H at 3360 cm^{-1}, while the O–H stretch appears as a singlet at 3569 cm^{-1} (see Table 2). As mentioned above, two sharp bands at 954 and 1065 cm^{-1} (labeled ε^a and ε^b, respectively) are most prominent when Gly resides at the C-terminus. The calculated spectra allow us to trace absorptions at these locations to the skeletal motions indicated by the displacement vectors of the corresponding normal modes presented in the inset of the figure. The band labeled (*) near 1340 cm^{-1} is not anticipated at the harmonic level, and is unique in that it is much broader than the others (30 versus ~10 cm^{-1}), suggesting that it may involve motion of the excess proton. Two transitions are actually calculated to be derived primarily from displacement of the H-bonded N–H stretch, one isolated at 2721 cm^{-1} and another near 1400 cm^{-1} (labeled IHB_a and IHB_b, respectively, in the lower trace of Figure 4). The former is conspicuously absent in the experimental spectrum while the observed bands near 1400 cm^{-1} appear significantly weaker than the calculated intensity of the H-bonded mode. The absence of these bands is readily explained by the anharmonicity associated with strongly shared protons in a variety of contexts [51–55], and is explicitly addressed in the context of all four systems in the Anharmonicity of the Intramolecular H-bond section.

Turning to the effect of methylation at the amide position, Figure 5 presents the predissociation spectrum (Figure 5a) obtained for $GlySarH^+\bullet(D_2)_2$ along with the calculated harmonic spectrum of the $GlySarH^+(1)$ minimum energy structure in Figure 5b. Qualitatively, methylation at the

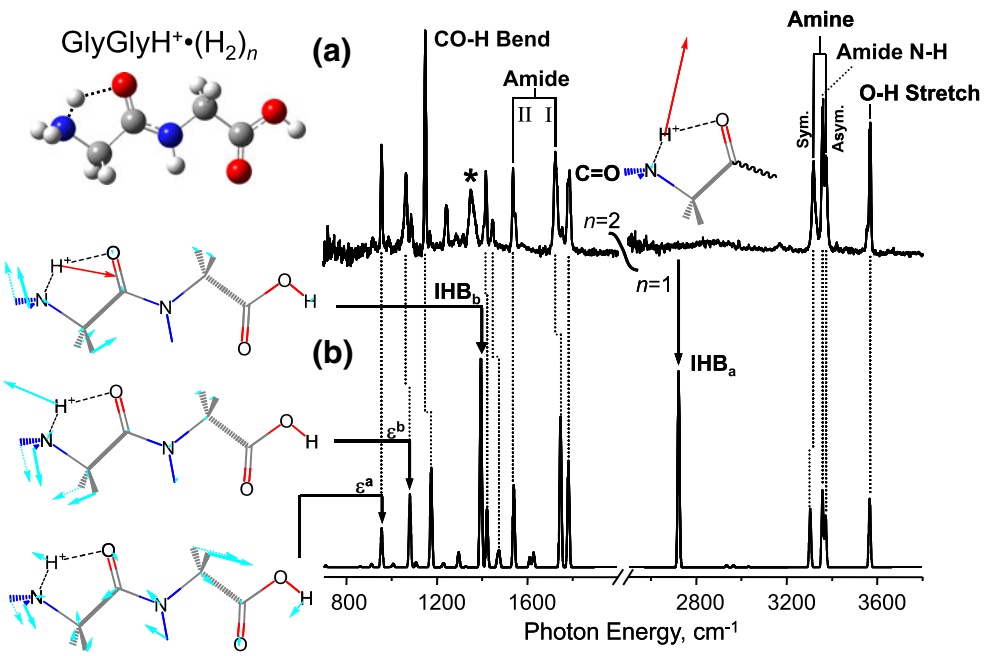

Figure 4. The vibrational predissociation spectrum of $GlyGlyH^+\bullet(H_2)_n$ **(a)** obtained by monitoring the loss of two H_2 molecules from the $n=2$ cluster below 2450 cm^{-1}, and by loss of one H_2 molecule from the $n=1$ cluster above 2450 cm^{-1}. Trace **(b)** displays the calculated harmonic spectrum (MP2/6-311 + G(d,p)) of the $GlyGlyH^+(1)$ structure (shown in the inset) scaled by factors of 0.943 and 0.977 above and below 2450 cm^{-1}, respectively, as described in the text. Displacement vectors are presented for the harmonic fundamentals, labeled IHB_a and IHB_b, which correspond to the modes mostly derived from the motion of the intramolecular H-bond. Displacement vectors are also presented for the low frequency normal modes calculated at 954 and 1065 cm^{-1}, labeled ε^a and ε^b, respectively, that involve a concerted motion of the peptide backbone with this structural motif

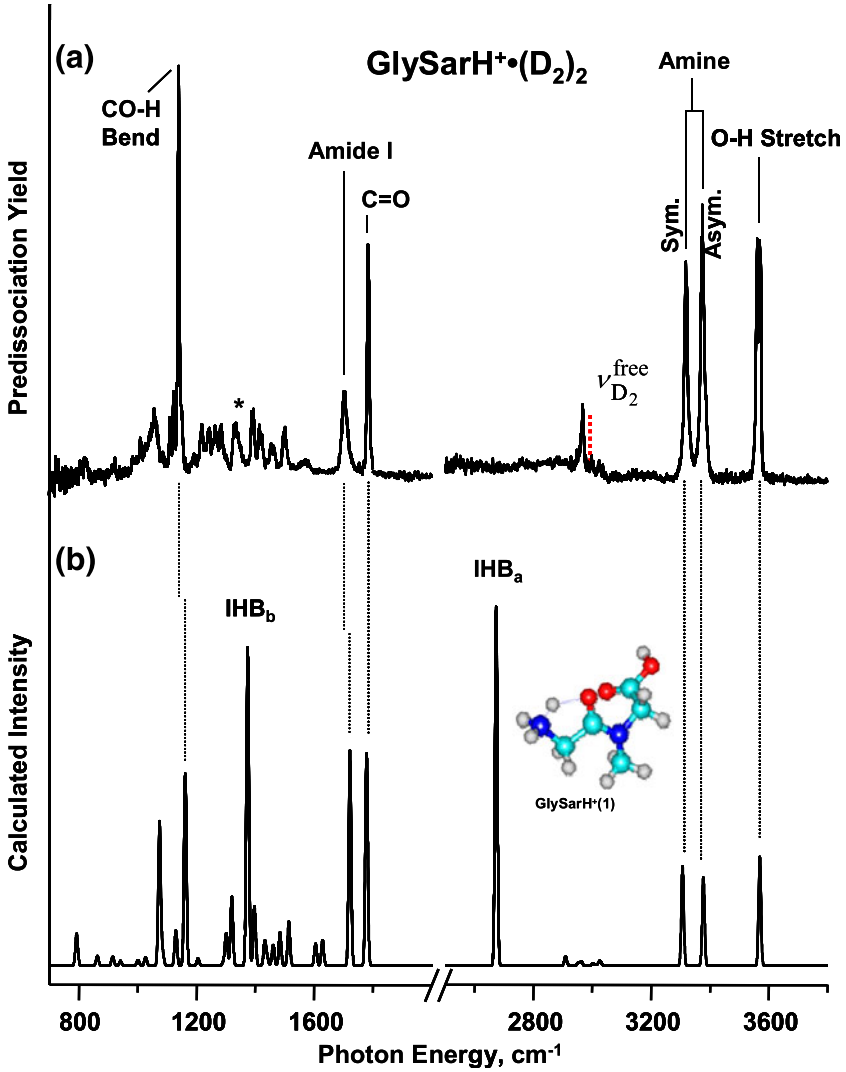

Figure 5. The vibrational predissociation spectrum of $GlySarH^+•(D_2)_2$ **(a)** obtained by monitoring the photoproduction of the bare protonated peptide. Trace **(b)** displays the calculated harmonic spectrum (MP2/6-311+G(d,p)) of the minimum energy $GlySarH^+$(1) isomer, scaled as described in the text

amide N–H in the center of the molecule should remove one of the three high frequency N–H stretches observed in the $GlyGlyH^+$ spectrum, since its amide band (Figure 2a) was observed to be nearly degenerate with the asymmetric NH_2 stretch of the amine near 3373 cm^{-1}. The latter feature occurs at 3375 cm^{-1} in the $GlySarH^+$ spectrum (Figure 2b and Figure 5a) and appears as a singlet with similar intensity to that of the lower energy symmetric NH_2 stretch at 3319 cm^{-1}, fully consistent with the expected loss of the amide N–H transition. The amide I band in $GlySarH^+$ appears red shifted (by 22 cm^{-1} to 1700 cm^{-1}) relative to that identified in $GlyGlyH^+$ (Figure 4), a modest perturbation consistent with its assignment mostly to the C=O stretching component of the amide group. On the other hand, the amide II mode in $GlyGlyH^+$ occurs at 1536 cm^{-1} and is primarily due to bending of the central N–H group, and as mentioned earlier, this band completely disappears when this amide hydrogen atom is replaced by CH_3 in the $GlySarH^+$ system. Instead, this region displays a series of weak transitions readily assigned to deformations of the CH_3 group around 1450 cm^{-1}.

Like the situation in $GlyGlyH^+$, the calculated harmonic spectrum of $GlySarH^+$(1) yields intense bands near 2700 and 1400 cm^{-1}, which are derived from harmonic motion of the intramolecular H-bonded proton in a similar cyclic motif. These bands are again absent in the experimental $GlySarH^+$ spectrum (Figure 5a). As in the spectrum of $GlyGlyH^+•(H_2)_2$, a band near 1340 cm^{-1} (labeled *) with similar width is present in the experimental spectrum of $GlySarH^+•(D_2)_2$, suggesting that both dipeptides yield this feature as a signature of their intramolecular H-bonds, a conjecture that will be developed further in the Anharmonicity of the Intramolecular H-bond section.

It is interesting to note the OH stretch at 3565 cm^{-1} occurs as a very close doublet with a splitting of 9 cm^{-1} (with expanded view in Figure S3). This observed splitting could possibly be caused by subtle changes in the local

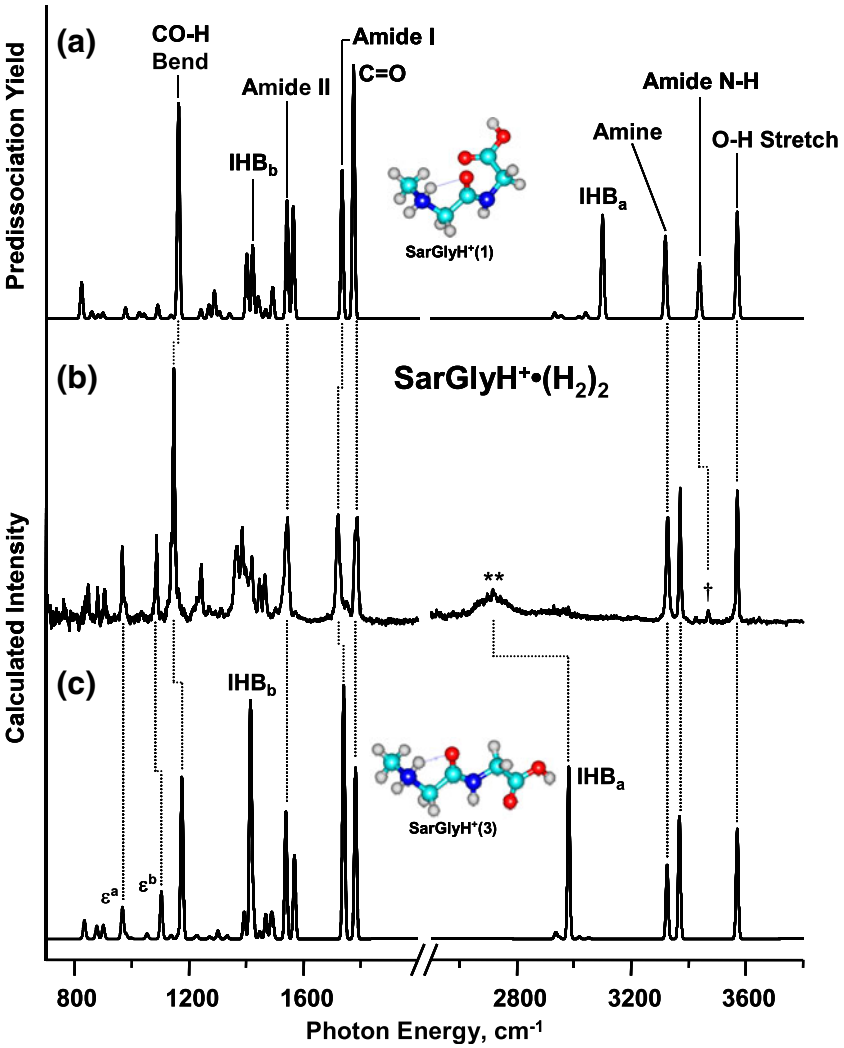

Figure 6. The vibrational predissociation spectrum of SarGlyH$^+$•(H$_2$)$_2$ **(b)** obtained by monitoring the photoproduction of the bare protonated peptide. Trace **(a)** and **(c)** display the calculated harmonic spectrum (MP2/6-311+G(d,p)) of the SarGlyH$^+$(1) and SarGlyH$^+$(3) isomers, respectively, scaled as described in the text

chemical environment of the O–H group. One likely scenario is that this doubling arises from a conformer generated by rotation about the amide bond (GlySarH$^+$(5) displayed in Figure S4e with harmonic spectrum in S5f), a modification that would cause minimal perturbation to the rest of the molecule. More extensive studies, for example those employing our isomer-selective double resonance technique [56], will likely be necessary to definitively establish the role of multiple isomers, and if indeed present, to reveal their independent spectral signatures. Other than the splitting of the OH stretch, most of the intense bands in the experimental spectrum can be readily assigned based on fundamentals derived from the minimum energy structure. Based on this analysis, we conclude that the predominant isomer is protonated on the amine in a fashion that accommodates formation of an intramolecular H-bond between the amino group and the amide oxygen. Note that this cyclic motif is very similar to that displayed by the minimum energy structure identified for GlyGlyH$^+$. Qualitatively, the main difference between GlyGlyH$^+$(1) and GlySarH$^+$(1) is that the latter undergoes significant rotation of the bond between amide nitrogen and the adjacent CH_2 group. This results in displacement of the acid group out of the plane of the molecule, presumably as a consequence of steric interaction with the methyl group at the amide position.

SarGlyH$^+$ and SarSarH$^+$

Both of these systems feature placement of the methyl group at the N-terminus. In the photodissociation spectrum of SarGlyH$^+$•(H$_2$)$_2$ (Figure 6b), we observe the presence of two intense bands in the N–H stretching region, one assigned to a free amine N–H stretch and the other to the characteristic amide N–H at 3370 cm^{-1}. The latter transition is only 10 cm^{-1} above the analogous band in the GlyGlyH$^+$ spectrum, confirming protonation on the secondary amine. Comparison of the observed bands with those predicted (Figure 6a) for SarGlyH$^+$(1) is particularly informative, as

the calculated position of the amide N–H stretch does *not* match the experimentally measured position. Moreover, two sharp bands observed at 967 and 1087 cm^{-1} are calculated to be much weaker than recovered experimentally. These two observations provide an important clue to identify the correct isomer in play as, based on the analysis of the $GlyGlyH^+$ spectrum, they were explained in the context of a collective motion along the backbone of an extended "all trans" structural motif. Indeed, the third lowest conformation identified, $SarGlyH^+(3)$, exhibits such an extended structure with its harmonic frequency spectrum presented in Figure 6c. The calculated amide N–H stretch and the extended ε^a and ε^b bands are now in good agreement with the experimental spectrum, thus suggesting that the MP2 methodology does not effectively describe the relative energies of this particular peptide. Interestingly, an analogous searching scheme utilizing the B3LYP methodology yielded the $SarGlyH^+(3)$ geometry as the lowest energy structure (Table S1). This highlights the ability of the H_2 tagging technique, which provides well resolved spectra over a wide frequency range, to identify subtle structural motifs in the face of contradictory theoretical predictions.

Turning to the $SarSarH^+$ spectrum highlighted in Figure 7a, we already noted the disappearance of both the amide N–H stretch and the asymmetric NH_2 stretch in the $SarSarH^+•(D_2)_2$ spectrum. The single strong N–H stretch that remains thus confirms protonation at the N-terminus. The calculated harmonic positions of the intense bands, such as the free amine N–H and C=O stretches of the $SarSarH^+(1)$ structure (Figure 7b) are in good agreement with the experimentally measured band positions. As in the case of $GlySarH^+$, the acid group is rotated out of the plane of the molecule in this structure, forming a twisted arrangement that still exhibits an IHB between the protonated amine and the amide oxygen. In the high energy stretching region, several minor features († in Figure 7a) again suggest the possible

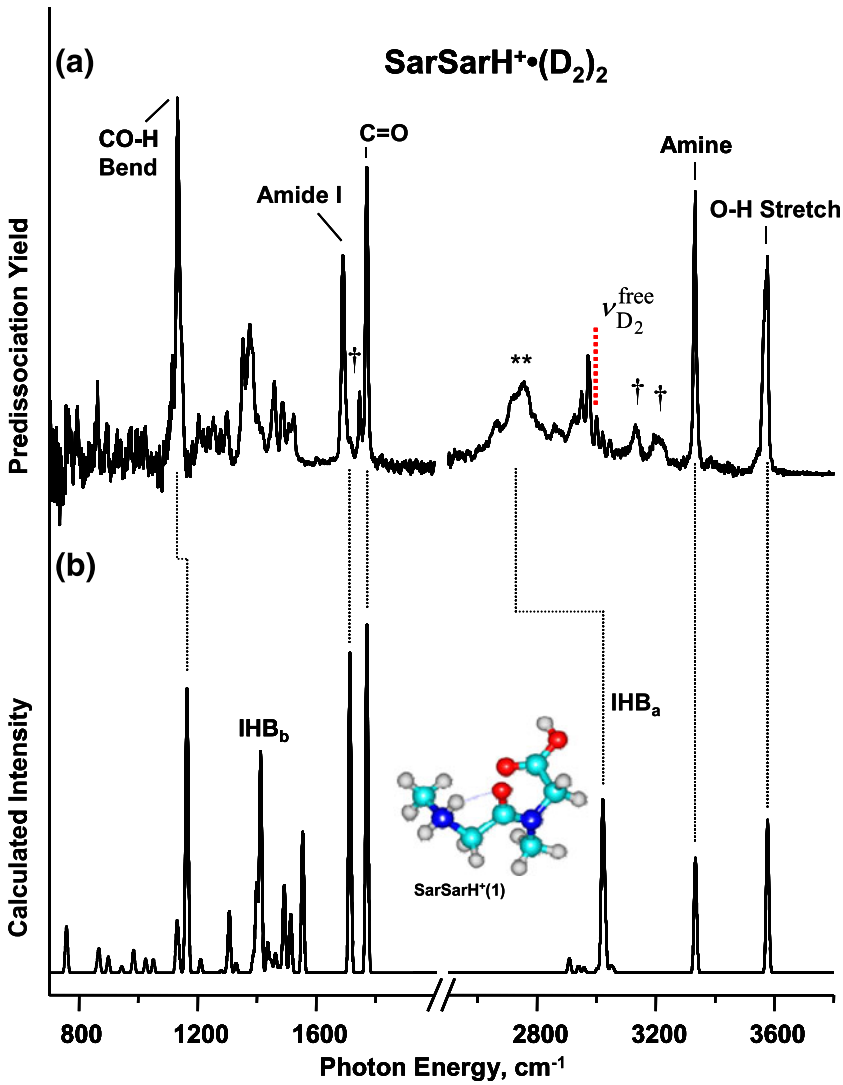

Figure 7. The vibrational predissociation spectrum of $SarSarH^+•(D_2)_2$ **(a)** obtained by monitoring the photoproduction of the bare protonated peptide. Trace **(b)** displays the calculated harmonic spectrum (MP2/6-311 + G(d,p)) of the minimum energy $SarSarH^+(1)$ isomer, scaled as described in the text

presence of additional isomers, but the dominant species is assigned to the minimum energy SarSarH$^+$(1) conformer.

In considering the nature of the intramolecular H-bond in the SarGlyH$^+$(3) and SarSarH$^+$(1) structures, we first note that methylation acts to increase the basicity associated with protonation of a secondary amine. This, in turn, should enhance localization of the excess proton on the amino functionality, and consequently reduce the strength of the intramolecular H-bond to the carbonyl [57]. This propensity is reflected in the harmonic spectra of SarGlyH$^+$(3) and SarSarH$^+$(1) (Figure 6c and Figure 7b), which predict the intramolecular H-bonded N–H stretches (labeled IHB$_a$) to occur 300 cm^{-1} higher in energy than those found with Gly as the N-terminal residue. Interestingly, the experimental spectra of both SarGlyH$^+$ and SarSarH$^+$ display very broad bands near 2700 cm^{-1} (denoted ** in Figure 2c and d), which are not present in either the GlyGlyH$^+$ or GlySarH$^+$ spectra. The (**) bands are thus strong candidates for assignment to IHB activity in both of these more basic systems.

Anharmonicity of the Intramolecular H-bond

To critically evaluate the assignment of the both the (*) and (**) bands to the intramolecular H-bond vibration, we carried out one-dimensional scans of the potential surfaces (MP2/6-311+G(d,p)) describing the displacement of the proton from donor N to the nearby acceptor O atom on the amide group, keeping all other atoms fixed at their equilibrium geometries. For all four peptides, we used the experimentally identified structures as the starting points. Scans were carried out by linearly displacing the mobile proton along a line connecting the coordinates that corresponded to protonation on the amino-N and amide-O. The resulting potential curves are displayed in Figure 8.

The calculated potential surfaces obtained for GlyGlyH$^+$(1) and GlySarH$^+$(1) are very similar, and exhibit a shallow minimum corresponding to protonation at the oxygen site. For GlyGlyH$^+$, relaxation of the latter structure in a second calculation, where all degrees of freedom were allowed to move, yielded a local minimum structure 5.2 kJ/mol (435 cm^{-1}) above the ground state with N–O and O–H distances of 2.488 and 1.022 Å, respectively. In the linear 1-D scans, the energy of the O-protonated structure is artificially increased due to the fact that the peptide backbone was frozen at the N-protonated geometry. Since the fully relaxed potential should depress the "shelf" region even lower in energy and involve much more collective action, it is therefore plausible that the (*) transition in GlyGlyH$^+$ and GlySarH$^+$ (the upper traces of Figure 4 and Figure 5) could arise primarily from the displacement of the internal H-bond.

As anticipated, the SarGlyH$^+$ (blue dotted line in Figure 8) and SarSarH$^+$ (black large-dashed line in Figure 8) potentials are considerably narrower, and display a much larger barrier for proton transfer to the amide oxygen compared with the two curves recovered with Gly at the N-terminus. These

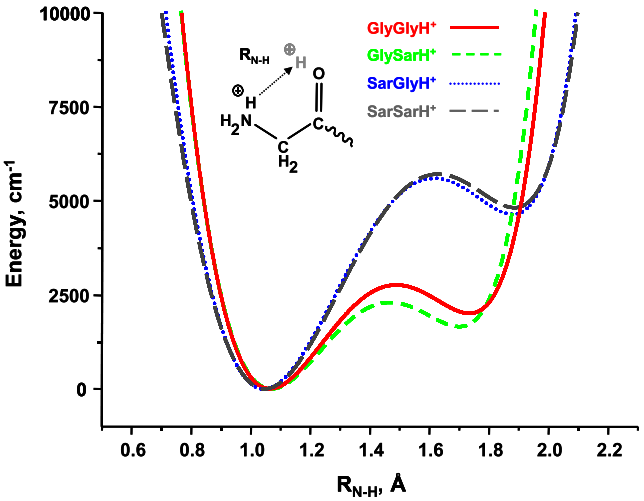

Figure 8. Potential energy traces (MP2/6-311+G(d,p)) for linear 1-D translational motion of the shared proton from the N-terminus to the amide carbonyl, with all other coordinates frozen at the N-protonated equilibrium geometry. The curves were shifted so as to bring all minima to the same energy

differences in shape lend support for the assignment of the broad bands near 2700 cm^{-1} (** in Figure 2c, d) to the intramolecular H-bonded N–H in both SarGlyH$^+$ and SarSarH$^+$. The blue-shift of the bands with increasing proton affinities of the binding sites is reminiscent of the behavior reported earlier for the trends in the H-bonded stretching frequencies in [A H$^+$ B] systems [51], where larger differences in proton affinities between donor and acceptor molecules gave rise to higher frequency bands.

Conclusion

A series of methylated dipeptides tagged with molecular hydrogen have been characterized using infrared predissociation spectroscopy and electronic structure calculations. All four systems accommodate the excess proton at the N-terminus and feature an intramolecular H-bond between the N atom and a nearby amide carbonyl. Strongly red-shifted, diffuse bands are assigned to displacements of hydrogen atoms involved in these intramolecular H-bonds with the aid of 1-dimensional cuts in the respective potential energy surfaces. The incorporation of a methyl group at the N-terminus results in a very large blue-shift in this H-bonded N–H stretch, an effect traced to the increased basicity of the substituted amino group. Methylation at the amide nitrogen in GlySarH$^+$ and SarSarH$^+$ appears to introduce a rotation of the C-terminus away from the backbone, in contrast to the species containing a secondary amide, GlyGlyH$^+$ and SarGlyH$^+$, which prefer an extended, "all trans" structure. Two low-energy transitions around 960 and 1065 cm^{-1} have been identified as signatures for conformers that adopt this extended arrangement. These results underscore the sensitivity of the intramolecular hydrogen bond to methylation at

two key positions, and illustrate the power of the H_2 tagging technique to expose these subtle structural changes.

Acknowledgments

M.A.J. thanks the National Science Foundation under grant CHE-091199 for support of this work, as well as the AFOSR under AFOSR award FA-9550-09-1-0139 for the cryogenic ion trap instrumental to the success of the H_2 tagging experiments. This work was supported in part by the Yale University Faculty of Arts and Sciences High Performance Computing facility (and staff). M.J.V.S. thanks the National Science Foundation under grant CHE-0239800. M.A.J. dedicates this paper to Albert R. Johnson in appreciation of his roles as a most excellent parent, mentor, and friend.

References

1. Mann, M., Aebersold, R.: Mass spectrometry-based proteomics. *Nature* **422**, 198–207 (2003)
2. Steen, H., Mann, M.: The ABC's (and XYZ's) of peptide sequencing. *Nature Rev. Mol. Cell Biol.* **5**, 699–711 (2004)
3. Papayannopoulos, I.A.: The interpretation of collision-induced dissociation tandem mass-spectra of peptides. *Mass Spectrom. Rev.* **14**, 49–73 (1995)
4. Wysocki, V.H., Tsaprailis, G., Smith, L.L., Breci, L.A.: Mobile and localized protons: A framework for understanding peptide dissociation. *J. Mass Spectrom.* **35**, 1399–1406 (2000)
5. Yalcin, T., Khouw, C., Csizmadia, I.G., Peterson, M.R., Harrison, A.G.: Why are B ions stable species in peptide spectra? *J. Am. Soc. Mass Spectrom.* **6**, 1165–1174 (1995)
6. Farrugia, J.M., O'Hair, R.A.J.: Involvement of salt bridges in a novel gas phase rearrangement of protonated arginine-containing dipeptides which precedes fragmentation. *Int. J. Mass Spectrom.* **222**, 229–242 (2003)
7. Bleiholder, C., Osburn, S., Williams, T.D., Suhai, S., Van Stipdonk, M., Harrison, A.G., Paizs, B.: Sequence-scrambling fragmentation pathways of protonated peptides. *J. Am. Chem. Soc.* **130**, 17774–17789 (2008)
8. Polfer, N.C., Oomens, J., Suhai, S., Paizs, B.: Infrared spectroscopy and theoretical studies on gas-phase protonated leu-enkephalin and its fragments: Direct experimental evidence for the mobile proton. *J. Am. Chem. Soc.* **129**, 5887–5897 (2007)
9. Bythell, B.J., Erlekam, U., Paizs, B., Maitre, P.: Infrared spectroscopy of fragments from doubly protonated tryptic peptides. *Chem. Phys. Chem.* **10**, 883–885 (2009)
10. Erlekam, U., Bythell, B.J., Scuderi, D., Van Stipdonk, M., Paizs, B., Maitre, P.: Infrared spectroscopy of fragments of protonated peptides: Direct evidence for macrocyclic structures of b(5) ions. *J. Am. Chem. Soc.* **131**, 11503–11508 (2009)
11. Chen, X., Steill, J.D., Oomens, J., Polfer, N.C.: Oxazolone versus macrocycle structures for leu-enkephalin b(2)-b(4): Insights from infrared multiple-photon dissociation spectroscopy and gas-phase hydrogen/deuterium exchange. *J. Am. Soc. Mass Spectrom.* **21**, 1313–1321 (2010)
12. Bythell, B.J., Maitre, P., Paizs, B.: Cyclization and rearrangement reactions of a(n) fragment ions of protonated peptides. *J. Am. Chem. Soc.* **132**, 14766–14779 (2010)
13. Molesworth, S., Leavitt, C.M., Groenewold, G.S., Oomens, J., Steill, J. D., van Stipdonk, M.: Spectroscopic evidence for mobilization of amide position protons during CID of model peptide ions. *J. Am. Soc. Mass Spectrom.* **20**, 1841–1845 (2009)
14. Simon, A., MacAleese, L., Maitre, P., Lemaire, J., McMahon, T.B.: Fingerprint vibrational spectra of protonated methyl esters of amino acids in the gas phase. *J. Am. Chem. Soc.* **129**, 2829–2840 (2007)
15. Wu, R., McMahon, T.B.: Infrared multiple photon dissociation spectroscopy as structural confirmation for GlyGlyGlyH(+) and AlaAlaAlaH(+) in the gas phase. Evidence for amide oxygen as the protonation site. *J. Am. Chem. Soc.* **129**, 11312–11313 (2007)
16. Wu, R.H., McMahon, T.B.: An investigation of protonation sites and conformations of protonated amino acids by IRMPD spectroscopy. *Chem. Phys. Chem.* **9**, 2826–2835 (2008)
17. Wu, R., McMahon, T.B.: Infrared multiple-photon dissociation mechanisms of peptides of glycine. *Chem. Eur. J.* **14**, 7765–7770 (2008)
18. Wu, R.H., McMahon, T.B.: Protonation sites and conformations of peptides of glycine ($Gly_{1\text{-}5}H^+$) by IRMPD spectroscopy. *J. Phys. Chem. B* **113**, 8767–8775 (2009)
19. Baquero, E.E., James, W.H., Choi, S.H., Gellman, S.H., Zwier, T.S.: Single-conformation ultraviolet and infrared spectroscopy of model synthetic foldamers: β-Peptides Ac-β(3)-hPhe-NHMe and Ac-β(3)-hTyr-NHMe. *J. Am. Chem. Soc.* **130**, 4784–4794 (2008)
20. Baquero, E.E., James, W.H., Choi, S.H., Gellman, S.H., Zwier, T.S.: Single-conformation ultraviolet and infrared spectroscopy of model synthetic foldamers: β-peptides Ac-β (3)-hPhe-β (3)-hAla-NHMe and Ac-β (3)-hAla-β (3)-hPhe-NHMe. *J. Am. Chem. Soc.* **130**, 4795–4807 (2008)
21. James III, W.H., Baquero, E.E., Shubert, V.A., Choi, S.H., Gellman, S.H., Zwier, T.S.: Single-conformation and diastereomer specific ultraviolet and infrared spectroscopy of model synthetic foldamers: ↦/β-Peptides. *J. Am. Chem. Soc.* **131**, 6574–6590 (2009)
22. Brenner, V., Piuzzi, F., Dimicoli, I., Tardivel, B., Mons, M.: Chirality-controlled formation of β-turn secondary structures in short peptide chains: Gas-phase experiment versus quantum chemistry. *Angew. Chem. Int. Ed.* **46**, 2463–2466 (2007)
23. Gloaguen, E., Pollet, R., Piuzzi, F., Tardivel, B., Mons, M.: Gas phase folding of an (Ala)(4) neutral peptide chain: Spectroscopic evidence for the formation of a β-Hairpin H-Bonding pattern. *Phys. Chem. Chem. Phys.* **11**, 11385–11388 (2009)
24. Abo-Riziq, A., Grace, L., Crews, B., Callahan, M.P., van Mourik, T., de Vries, M.S.: Conformational Structure of Tyrosine, Tyrosyl-glycine, and Tyrosyl-glycyl-glycine by Double Resonance Spectroscopy. *J. Phys. Chem. A* ASAP, 10.1021/jp110601w (2011)
25. Vaden, T.D., de Boer, T.S.J.A., Simons, J.P., Snoek, L.C., Suhai, S., Paizs, B.: Vibrational spectroscopy and conformational structure of protonated polyalanine peptides isolated in the gas phase. *J. Phys. Chem. A* **112**, 4608–4616 (2008)
26. Vaden, T.D., de Boer, T.S.J.A., Simons, J.P., Snoek, L.C.: Intramolecular interactions in protonated peptides: H^+PheGlyGly and H^+GlyGlyPhe. *Phys. Chem. Chem. Phys.* **10**, 1443–1447 (2008)
27. Wang, D., Gulyuz, K., Stedwell, C.N., Polfer, N.C.: Diagnostic NH and OH Vibrations for Oxazolone and Diketopiperazine Structures: b2 from Protonated Triglycine. *J. Am. Soc. Mass Spectrom.* **ASAP**, 10.1007/S13361-13011-10147-13363 (2011)
28. Forbes, M.W., Bush, M.F., Polfer, N.C., Oomens, J., Dunbar, R.C., Williams, E.R., Jockusch, R.A.: Infrared spectroscopy of arginine cation complexes: Direct observation of gas-phase zwitterions. *J. Phys. Chem. A* **111**, 11759–11770 (2007)
29. Vaden, T.D., Gowers, S.A.N., de Boer, T.S.J.A., Steill, J.D., Oomens, J., Snoek, L.C.: Conformational preferences of an amyloidogenic peptide: IR spectroscopy of Ac-VQIVYK-NHMe. *J. Am. Chem. Soc.* **130**, 14640–14650 (2008)
30. Dunbar, R.C., Steill, J.D., Polfer, N.C., Oomens, J.: Gas-phase infrared spectroscopy of the protonated dipeptides H(+)PheAla and H(+)AlaPhe compared with condensed-phase results. *Int. J. Mass Spectrom.* **283**, 77–84 (2009)
31. Rajabi, K., Fridgen, T.D.: Structures of aliphatic amino acid proton-bound dimers by infrared multiple photon dissociation spectroscopy in the 700–2000 cm^{-1} region. *J. Phys. Chem. A* **112**, 23–30 (2008)
32. Polfer, N.C., Oomens, J.: Vibrational spectroscopy of bare and solvated ionic complexes of biological relevance. *Mass Spec. Rev.* **28**, 468–494 (2009)
33. Kupser, P., Pagel, K., Oomens, J., Polfer, N., Koksch, B., Meijer, G., von Helden, G.: Amide-I and -II vibrations of the cyclic β-sheet model peptide gramicidin S in the gas phase. *J. Am. Chem. Soc.* **132**, 2085–2093 (2010)
34. Kamrath, M.Z., Garand, E., Jordan, P.A., Leavitt, C.M., Wolk, A.B., Van Stipdonk, M.J., Miller, S.J., Johnson, M.A.: Vibrational characterization of simple peptides using cryogenic infrared photodissociation of H_2-tagged, mass-selected ions. *J. Am. Chem. Soc.* **133**, 6440–6448 (2011)
35. Stearns, J.A., Boyarkin, O.V., Rizzo, T.R.: Spectroscopic signatures of gas-phase helices: Ac-Phe-(Ala)(5)-Lys-H+and Ac-Phe-(Ala)(10)-Lys-H+. *J. Am. Chem. Soc.* **129**, 13820 (2007)

36. Stearns, J.A., Seaiby, C., Boyarkin, O.V., Rizzo, T.R.: Spectroscopy and conformational preferences of gas-phase helices. *Phys. Chem. Chem. Phys.* **11**, 125–132 (2009)
37. Nagornova, N.S., Rizzo, T.R., Boyarkin, O.V.: Highly Resolved Spectra of Gas-Phase Gramicidin S: a Benchmark for Peptide Structure Calculations. *J. Am. Chem. Soc.* **132,** 4040-+(2010)
38. Goebbert, D.J., Wende, T., Bergmann, R., Meijer, G., Asmis, K.R.: Messenger-tagging electrosprayed ions: Vibrational spectroscopy of suberate dianions. *J. Phys. Chem. A* **113**, 5874–5880 (2009)
39. Jiang, L., Wende, T., Bergmann, R., Meijer, G., Asmis, K.R.: Gas-phase vibrational spectroscopy of microhydrated magnesium nitrate ions $[MgNO_3(H_2O)_{1-4}]^+$. *J. Am. Chem. Soc.* **132**, 7398–7404 (2010)
40. Wang, X.B., Xing, X.P., Wang, L.S.: Observation of H_2 aggregation onto a doubly charged anion in a temperature-controlled ion trap. *J. Phys. Chem. A* **112**, 13271–13274 (2008)
41. Okumura, M., Yeh, L.I., Myers, J.D., Lee, Y.T.: Infrared spectra of the cluster ions $H_7O_3^+ \cdot H_2$ and $H_9O_4^+ \cdot H_2$. *J. Chem. Phys.* **85**, 2328–2329 (1986)
42. Okumura, M., Yeh, L.I., Myers, J.D., Lee, Y.T.: Infrared-spectra of the solvated hydronium ion: Vibrational predissociation spectroscopy of mass-selected $H_3O^+ \cdot (H_2O)_n \cdot (H_2)_m$. *J. Phys. Chem.* **94**, 3416–3427 (1990)
43. Campbell, S., Rodgers, M.T., Marzluff, E.M., Beauchamp, J.L.: Deuterium exchange reactions as a probe of biomolecule structure. Fundamental studies of gas phase H/D exchange reactions of protonated glycine oligomers with D2O, CD3OD, and CD3CO2D, and ND3. *J. Am. Chem. Soc.* **117**, 12840–12854 (1995)
44. He, F., Marshall, A.G., Freitas, M.A.: Assignment of gas-phase dipeptide amide hydrogen exchange rate constants by site-specific substitution: GlyGly. *J. Phys. Chem. B* **105**, 2244–2249 (2001)
45. Wu, J.Y., Lebrilla, C.B.: Gas-phase basicities and sites of protonation of glycine oligomers (Glyn, N=1–5). *J. Am. Chem. Soc.* **115**, 3270–3275 (1993)
46. Wang, X.B., Wang, L.S.: Development of a low-temperature photoelectron spectroscopy instrument using an electrospray ion source and a cryogenically controlled ion trap. *Rev. Sci. Instrum.* **79**, 073101–073108 (2008)
47. Kamrath, M.Z., Relph, R.A., Guasco, T.L., Leavitt, C.M., Johnson, M. A.: Vibrational predissociation spectroscopy of the H2-tagged mono- and dicarboxylate anions of dodecanedioic acid. *Int. J. Mass Spec.* **300**, 91–98 (2011)
48. Jorgensen, W.L., Tirado-Rives, J.: Molecular modeling of organic and biomolecular systems using BOSS and MCPRO. *J. Comp. Chem.* **26**, 1689–1700 (2005)
49. Frisch, M.J., Trucks, G.W., Schlegel, H.B., Scuseria, G.E., Robb, M.A., Cheeseman, J.R., Scalmani, G., Barone, V., Mennucci, B., Petersson, G. A., Nakatsuji, H., Caricato, M., Li, X., Hratchian, H.P., Izmaylov, A.F., Bloino, J., Zheng, G., Sonnenberg, J.L., Hada, M., Ehara, M., Toyota, K., Fukuda, R., Hasegawa, J., Ishida, M., Nakajima, T., Honda, Y., Kitao, O., Nakai, H., Vreven, T., J.A. Montgomery, J., Peralta, J.E., Ogliaro, F., Bearpark, M., Heyd, J.J., Brothers, E., Kudin, K.N., Staroverov, V.N., Kobayashi, R., Normand, J., Raghavachari, K., Rendell, A., Burant, J.C., Iyengar, S.S., Tomasi, J., Cossi, M., Rega, N., Millam, J.M., Klene, M., Knox, J.E., Cross, J.B., Bakken, V., Adamo, C., Jaramillo, J., Gomperts, R., Stratmann, R.E., Yazyev, O., Austin, A.J., Cammi, R., Pomelli, C., Ochterski, J.W., Martin, R.L., Morokuma, K., Zakrzewski, V.G., Voth, G.A., Salvador, P., Dannenberg, J.J., Dapprich, S., Daniels, A.D., Farkas, Ö., Foresman, J.B., Ortiz, J.V., Cioslowski, J., Fox, D.J.: Gaussian 09, Revision A.02. *Gaussian, Inc., Wallingford, CT.* (2009)
50. NIST Computational Chemistry Comparison and Benchmark Database, N. S. R. D. N., Release 15a, April 2010, Editor: Russell D. Johnson III, http://cccbdb.nist.gov/
51. Roscioli, J.R., McCunn, L.R., Johnson, M.A.: Quantum structure of the intermolecular proton bond. *Science* **316**, 249–254 (2007)
52. Gardenier, G.H., Roscioli, J.R., Johnson, M.A.: Intermolecular proton binding in the presence of a large electric dipole: Ar-tagged vibrational predissociation spectroscopy of the $CH_3CN \cdot H^+ \cdot OH_2$ and $CH_3CN \cdot D^+ \cdot OD_2$ complexes. *J. Phys. Chem. A* **112**, 12022–12026 (2008)
53. Hammer, N.I., Diken, E.G., Roscioli, J.R., Johnson, M.A., Myshakin, E. M., Jordan, K.D., McCoy, A.B., Huang, X., Bowman, J.M., Carter, S.: Vibrational predissociation spectra of the $H_5O_2^+ \cdot RG_n$ (RG=Ar, Ne) clusters: Correlation of the solvent perturbations in the free OH and shared proton transitions of the zundel ion. *J. Chem. Phys.* **122**, 244301 (2005)
54. Ricks, A.M., Douberly, G.E., Duncan, M.A.: Infrared spectroscopy of the protonated nitrogen dimer: The complexity of shared proton vibrations. *J. Chem. Phys.* **131**, 104312 (2009)
55. Douberly, G.E., Ricks, A.M., Ticknor, B.W., Duncan, M.A.: Structure of protonated carbon dioxide clusters: Infrared photodissociation spectroscopy and Ab initio calculations. *J. Phys. Chem. A* **112**, 950–959 (2008)
56. Elliott, B.M., Relph, R.A., Roscioli, J.R., Bopp, J.C., Gardenier, G.H., Guasco, T.L., Johnson, M.A.: Isolating the spectra of cluster ion isomers using Ar-"Tag"-Mediated IR-IR double resonance within the vibrational manifolds: Application to $NO_2^- \cdot H_2O$. *J. Chem. Phys.* **129**, 094303 (2008)
57. Jeffrey, G.A.: An Introduction to Hydrogen Bonding, p. 220–225. Oxford University Press, New York (1997)